Multiple Driver Modeling with a Modern Lumped Element Simulation Program

Jörg W. Panzer, Panzer and Partner
Steinstr. 15, D-81667 Munich, Germany
and
Richard H. Campbell
Worcester Polytechnic Institute
100 Institute Rd., Worcester, MA 01609, USA

Abstract

The dodecahedron loudspeaker, a design widely used in acoustic measurements, is modeled using components available in a computer-based electroacoustic network simulator. The acoustic radiation and driver behavior simulation includes specifying the physical position and radiation angle of each of the twelve drivers. Comparison is made with anechoic chamber measurements on a real loudspeaker.

0. Introduction

This paper demonstrates the simulation of the response involving multiple drivers mounted on the surface of a spherical body radiating in all directions. This special loudspeaker design is widely used in acoustic measurements where it serves as an omnidirectional sound source. The simulation of the transfer and loading parameters not only helps in designing such a loudspeaker but also the simulation leads to a sound understanding of the fundamental effects. The paper also explains how the classical lumped element method can be applied successfully using an analyzer for electroacoustical networks. The analyzer used is an available computer program called AkAbak® running under Windows™ 3.x.

1. Loudspeaker enclosure

The radiators in the system under study are mounted each in the center of the 12 faces of a regular dodecahedron. The dodecahedron is a so-called Platonic body (Fig. 1) consisting of 12 regular pentagons joined at their edges. Due to the regular form and high number of faces the dodecahedron is acoustically a close approximation to the radiation from a sphere.

Table 1 Driver parameter

Eff. outer diaphragm diameter dD	93.5 mm	
Eff inner diameter dD1	30 mm	
Depth of cone tD1	11 mm	
Frequency of mass reduction fp	4.5 kHz	
Mass of vibrating assembly Mms	4.95 g	(incl. air load)
Compliance of suspension Cms	0.6 mm/N	
Motor conversion factor Bl	2.1 Tm	
Voice coil resistance Re	0.93 Ω	
Voice coil inductance factor Le	120 µH	(approx. "squared reactance")

2. Loudspeaker drive units

There are 12 equal drive units. Each driver has an electro- dynamical motor and a conical shaped diaphragm. The parameters of the diaphragm and the motor are given in Table 1. The mass of the vibrating assembly together with the suspension compliance yield to a fundamental free field resonance of fs=92Hz. The parameter of the frequency of mass reduction fp is used by the simulator to take into account that at high frequencies only part of the diaphragm radiates sound.

The voice coil reactance differs from the curve of a pure inductance. A good approximation is to take the square root: $Xe(j\omega)=sqrt(\omega Le)$. This is not exactly what the simulator does, but without going into details here, it is a good way to understand this specification in principal.

3. The simulator

The simulator used is a Windows™ program called AkAbak which is a synonym for "Acoustic Abakus". This software provides an integrated development system for analyzing and designing electroacoustic devices such as loudspeaker drivers and systems.

To be able to describe the structure under investigation by means of AkAbak, the structure must be first separated into a set of lumped elements and one-dimensional waveguides. The components are wired with a

node-based system, called a network. Based on linear system theory, the analysis is carried out in the frequency domain by solving the node-potential-matrix.
AkAbak offers special components which are dedicated to especially loudspeaker design. There are several complete models for transducers, waveguides, enclosures and radiation which are used to simulate the response when multiple radiation sources are involved.
Before arranging all of the components into a full system it is necessary to understand how AkAbak handles the radiation of cone shaped diaphragms, and other computational aspects of the simulator.

4. Loading and radiation into free space

4.1 Self-radiation impedance

Each diaphragm is acoustically loaded by the so-called radiation impedance. The radiation impedance is the ratio of the driving velocity of the air in the very near of the diaphragm surface and the pressure reacting back onto it. If we imagine us the diaphragm surface separated into many small sub-areas then the force on one of this sub-areas is created by the generated sound pressure of all the other sub-areas. The total self-radiation impedance is then obtained by surface-integration over the diaphragm.
The acoustical power output is proportional to the real part of the radiation impedance, Re(Z_A). The impedance function, Re(Z_A), resembles that of a high-pass filter having a typical cut-off frequency where one wavelength of the radiated sound is equal to the perimeter of the circular diaphragm. This frequency is sometimes called the *directivity frequency*, fD, or the *rim resonance*. In Figure 2 the directivity frequency is at approx. fD=1.2kHz.

The magic of flat direct-loudspeaker response lies in the cooperation of the velocity of the diaphragm and the radiation resistance (Fig. 3). The band-pass curve of the velocity is centered at the fundamental resonance of the driver. At frequencies above this point, the so-called mass controlled region, the roll-off of the velocity curve is compensated with respect to the radiated power by the rising radiation resistance. Above the directivity frequency, fD, where the radiation resistance is approximately constant, the well known drop of the power output can be recognized.

Cones, which belong to the class of concave-formed diaphragms, cause standing wave patterns to exist which increases the radiation impedance. The strongest effect on the power output is caused by an amplification of the radiation resistance in the region of the directivity frequency, fD (Fig. 2). Nearly all cone shaped diaphragms have an enhanced power response in the vicinity of the directivity frequency (Fig. 4).
Near and above the directivity frequency mechanical eigen-vibration of the diaphragm also effects the radiation impedance. Without going into details one major effect can be extracted. With rising frequency the acceleration of the whole vibrating assembly is so strong that only a part of the diaphragm comes into controlled motion. To be able to simulate this reduction of radiating area and vibrating mass in principal, we use the estimation parameter fp. The frequency fp can be regarded as a cut off frequency where only half of the cone-diaphragm area is vibrating. At higher frequencies the radiating part of the cone becomes smaller until only a small ring around the voice coil is radiating.

4.2 Mutual-radiation impedance

The force, reacting back to any point of the diaphragm surface, naturally can be caused by any other radiating source, in the same way as the diaphragm does it to itself. This source can be any other driver or reflecting wall as well. Within the latter is included the baffle in which the diaphragm is mounted.
The mutual-radiation impedance between diaphragms can be understood in the same way as the self-radiation impedance. The sound pressure radiated to each sub-area of the other diaphragm creates a force there forming part of the total radiation impedance.
The closer the other radiator is the stronger is the coupling. The strongest coupling is exhibited by the baffle in which the diaphragm is mounted. An infinite baffle doubles the radiation resistance. A finite baffle causes diffraction at the baffle edges. At high frequencies the radiation resistance is double the amount as at low frequencies.
The simulator implements a radiation impedance element in the network which takes into account mutual coupling caused by reflecting walls and by the baffle including diffraction effects. The effects of the feedback of the mutual coupling into the network is usually very small because of the extremely low acoustical energy which is received when radiation takes place in free space.

4.3 Radiation

The sound pressure at any listing point outside the source is the sum-total of generated sound of all diaphragms including diffraction and reflections.

4.3.1 Radiation of diaphragm
Because the dimension of a single diaphragm is within the range of the radiated wavelength, an interference phenomenon causes the well-known directivity or beaming effect (Fig. 5). Consider that if the diaphragm

surface separated into many small sub-areas, the pathlength from each of this sub-areas to the listening point is different. When this difference is comparable to the wavelength or greater interference occurs. When the listening point is sufficiently far away from the source the rays from the radiating surfaces to the listing point can be regarded parallel, a condition known as far-field. For example, a piston-like diaphragm will cause no interference on-axis in the far-field. But when the test point is moved off-axis, interference of the closer and more far away sub-areas of the diaphragm causes directivity or a drop of output power, respectively.
Diaphragm shapes other then the piston will exhibit interference in the far-field even on-axis. The reason for this is that the radiating sub-areas of the vibrating diaphragm are not all located in the plane normal to the direction of the listening point.
The simulator calculates the directivity of a single diaphragm in the far field and takes into account the form of the diaphragm. The cone is divided into many rings. From each ring the directivity is calculated and then numerically integrated over the entire surface of the diaphragm. The integration limits are derived from the effective diaphragm area which is frequency dependent as mentioned earlier. Compared to a rigid diaphragm the directivity of a frequency controlled diaphragm decreases at high frequencies (Fig. 5).

4.3.2 Diffraction at the baffle edges
The finite baffle size causes diffraction. The sound pressure level is twice as high at high frequencies than at low frequencies (Fig. 6). The fundamental effect of diffraction is interference. Using a simplified model imagine the finite baffle formed of two parts: the actual baffle in which the diaphragm is mounted, and the extended area behind the edges in the same plane as the baffle itself. As soon as the traveling wave is behind the edges a pressure gradient is produced toward the reverse side of the baffle, thus creating a second radiator. The sound generated by this "outer" diaphragm adds to the direct radiated sound of the source, but it is time delayed.
The simulator calculates the diffraction effects using the mirror model. For the "outer" diaphragm one or two additional radiators are installed by the program. Only one mirror radiator is needed when the baffle edges are approximately equidistant from the source diaphragm. A second mirror radiator is added when the baffle is rectangular or the source is mounted asymmetrically. The mirror-radiators are fed a time-delayed signal by the source and with a radiation angle of 90°. With this arrangement and because every diaphragm possesses directivity, the diffraction effect is diminished at high frequencies, which is exactly what we observe on real baffles. At high frequencies the diaphragm becomes its own baffle.
This simple implementation of the diffraction effect leads to surprisingly good results and is a good compromise between exactness, calculation speed and parameter specification.

4.3.3 Reflection
There are two cases of reflection simulated by AkAbak. Firstly, the main reflector is always the baffle in which the diaphragm is mounted or at high frequencies the diaphragm itself. Secondly, depending on the wavelength, a sufficiently large and rigid wall distant to the source will cause interference due to the traveling time of the sound wave from the source to the reflector and from the reflector to the listening point. In the first case the reflected wave interferes with the source modifying the radiation impedance. In the second case the reflected wave interferes with the direct radiated sound at the listing point. In closed listening rooms, a standing wave pattern further modifies the radiation impedance and the observed sound at the listening point.
AkAbak takes into account a maximum of three orthogonal reflecting walls affecting the radiation impedance and the radiated sound, again using the mirror radiator model. For each wall and for each original source additional mirror radiators of first, second and third order are installed automatically.

4.4 Radiation from multiple sources

When multiple radiators are involved the sum-total of complex sound pressure of all radiators including diffraction and reflection is summed at the listing point.
In the simulation-result the sum-total of sound pressure of all radiators is a near-field condition and a far-field condition with respect to the radiation of a single diaphragm.
The acoustical power output of the assembly is obtained by surface-integration over a sphere outside the loudspeaker.
To be able to calculate the directivity and the level with respect to the listening point the exact position and mounting angle of each radiator must be specified. Further it is required to provide entries for the effective baffle size and the distance and specification of the reflecting walls.

5 Loading and radiation into the enclosure

The reverse side of the diaphragm is usually loaded by an enclosure. The acoustics of small enclosures, where the dimension of the enclosure is of the order of a wavelength, is totally different from the radiation into free space. The standing wave-pattern in normal loudspeaker enclosures can be categorized in three frequency ranges. In the low frequency range, where the wavelength is much larger then the dimensions of the enclosure, the air in the cavity is reacting like a spring and a small mass to an applied force. In the medium frequency range, where the wavelength is in the range of the largest extent of the enclosure the cavity can be regarded as

an one-dimensional waveguide. In the high frequency range, the wave-equation must be solved with time dependency in all dimensions.
Beside the simple closed rectangular cavity the enclosure can be of any form. It may be tube or horn like, with bends and obstacles. There might be multiple driving (or passive) diaphragms or radiating holes.
To simulate the acoustic response of such applications with lumped elements and one-dimensional waveguides it is necessary to investigate and separate the structure into modules. These modules are then interconnected in a network similar to the analysis of electric circuits. Because of the reflecting boundaries the sound pressure within an enclosure is usually much higher than in free space. In simulations careful investigation is necessary to be certain that linear system theory is still valid at high levels.
In the docecahedron loudspeaker 12 diaphragms are radiating in the same small closed enclosure of nearly spherical form. Naturally this form is impossible to separate exactly into three independent dimensions and because of this one can only approximate the exact acoustic wave-pattern inside the enclosure. At low frequencies the air reacts like a spring to all diaphragms. At approx. 700 Hz the first eigen-frequency of the cavity appears and modifies the loading of the drivers. At high frequencies multiple modes spread all over the inner of the enclosure to amplify and damp one or the other driver. Fortunately the higher modes have much less energy at a single point then the fundamental and because of this their effect can be seen as small peaks and dips in the curves.
In this simulation we model the enclosure with Duct-components as an approximation of the three dimensional wavefield. The Duct element is a one-dimensional waveguide with constant cross-section. We connect the Duct-fourpoles in a star-like arrangement with one port of each Duct connected with the reverse side of each diaphragm. The other end is connected with all other Ducts to an Enclosure element in the center of the star. The cross-section and length of each of the 12 Ducts are derived from the effective inner volume and dodecahedron dimensions. The Enclosure element itself is also a single waveguide taking into account the fundamental mode in the largest dimension. It is vented here to model some losses which are apparently present due to air leaks between the driver flange and the enclosure shell. In this way not only the correct loading but also the interaction of opposite-located drivers is maintained.

6. Data specification and simulation

AkAbak's input system is a text script edited by an built-in word-processor (see addendum). The elements are written in paragraphs. The parameters can be entered as a constant value or in the form of a formula system. Node-numbers connect the components. Drivers must be specified at the beginning of the script and are then used in the networks as often as needed.
In this example, most of the parameters in the acoustical network portion of the dodecahedron loudspeaker depend on the geometry of the Platonic body. Therefore, the Def_Const definition at the beginning of the script is used to calculate all the needed positions, mounting angles and parameters of the duct elements of the enclosure. In this way it is easy to control the input of many elements by only one or two stated variables. The specification starts with the edge length of the pentagonal face. In this way, the response of a larger or smaller dodecahedron loudspeaker can be computed simply by altering one value.
After entering all data, the script is compiled into binary format and then the spectrum analysis is carried out. There are numerous ways of inspecting the network and displaying the simulation. A loudspeaker should always be simulated at least at its input and output port. Figure 8 to 11 are examples for several simulations including measurement curves. The measurements are carried out in a sound absorbing chamber using the MLSSA system, DRA Laboratories, USA.
The drivers are mounted in such a way that one of the diaphragms has its mounting point on the z-axis. The z-axis of the baffle coordinate system is the "on-axis" reference. The y-axis points upwards and the x-axis to the left of the baffle (seen from the baffle). The distance to the listening point is measured from the center of the dodecahedron, i.e. six speakers are offset toward the on-axis listening point and six speakers are positioned behind the origin facing rearward.
One of the advantages of the lumped element simulation is the high calculation speed. For example, it takes about two minutes on a modern PC to compile and calculate the extensive script given in the addendum and the spectrum of Figure 9 with a high resolution.
Figure 11 displays the sound power output (SWL) calculated by surface integration. The other graph is the on-axis SPL. The third is the directivity factor Q relating to the on-axis response (abbreviated). The directivity factor is Q = 1 at low frequencies and rises at high frequencies due to power loss caused by interference. Both curves are under free field condition without any reflector. Note that the SPL drops by 6 dB but the SWL only by 3 dB radiating into 4π space.

6. Discussion

A lumped element simulator is a computer-aided design tool which helps to investigate, understand and enhance a loudspeaker system. The lumped element method is simple, but forces an understanding of the structure under investigation. Because it concentrates exclusively on the main effects, this analysis method is both practical and fast.

In the real world, resonance points and interference effects are more or less unsharp, damped or distorted. Because AkAbak uses only a limited set of components, resonances and interference effects are displayed with more pronounced effect. To the loudspeaker designer, the curves might be not so pleasant at first glance but highly informative.

The simulation of the dodecahedron loudspeaker reveals an interesting effect which can be worked out with this analysis method.
Seen from the on-axis listening point the centers of the 12 diaphragms are located in four planes. On the nearest plane one speaker is mounted. In the next plane five speakers are arranged in a circle around the z-axis radiating toward the side. On third plane five loudspeakers radiate rearward to the side, and on the last plane a single driver is opposite to the front speaker. Because of the regular offset a sharp interference occurs on-axis which can be seen clearly in the SPL curve of Figure 9 (1.3 kHz).
Oddly enough, another resonance at the same frequency seems to compensate the notch. This resonance is produced by the 2nd eigen-frequency of the enclosure modifying the acoustical load of the drivers. The next mode is at 2.6 kHz. In the simulation script the length of the Ducts which model the enclosure is directly derived from the dodecahedral geometry. The length of each Duct is equal to the radius of an inscribed sphere (Constant "b" in the Def_Const specification of the script).

It is essential to compare the simulation with both the measurement of a transfer function and the measurement of a driving point parameter. Here the transfer function is the SPL curve and the driving point is the electrical impedance curve. The curves in Figure 8 have multiple peaks. The pronounced one at approx. 250 Hz belongs to the mechanical resonance of the drivers. The peak below is caused by leakages of the enclosure which makes it actually a lossy, vented box. In reality the losses are more smeared with respect to frequency. At 700 Hz and 1.3 kHz the varying acoustic load on the drivers caused by the standing waves in the enclosure are fedback to the motional impedance.

Investigating the time domain response, a further interesting result can be obtained. From the spectrum the so-called energy time curve (ETC) can be calculated. The ETC is the magnitude of the analytical time transfer function. Derived from the SPL spectrum, it displays the time arrival of acoustic energy at the listening point. Figure 12 compares the ETC curves of a single driver and of the whole assembly. The peaks belong to the different driver mounting offsets. When only the front driver is radiating (which is only possible in the simulation) all energy is concentrated at approximately -330µs (calculated from the baffle origin). When all drivers are radiating, a cascade of sound energy arrives at the listening point carrying the same information. The result is a noticeably smeared time signal.

It is proper to say that the dodecahedron has omnidirectional radiation, but it is improper to say that it has spherical radiation characteristics. Even if an ever increasing multiplicity of faces and drivers were used, in the limit leading to an essentially spherical radiating surface, the presense of the hard shell causes unavoidable diffraction and interference from the spatial radiatiing elements distributed around its surface. An expanding spherical wave (with the same radius of curvature) in free space which originated at a point, has no shell and no diffraction, and no arrival time smear.

7. Conclusion

The coupling of a powerful calculation module to an accurate acoustic modeling program has significant benefits as seen in this paper. The translation and rotation of the 12 drivers as well as certain volume and diffraction values are all calculated from an embedded script which has a single given value at the begining -- the length of one edge of a pentagonal face. This same technique can be used to develop complex horn shapes using piece-wise linear segments.

8. References

1. Hill, F. S.: "Computer Graphics", Collier Macmillian Canada Inc.
2. Beranek, L. L.: “Acoustics”; American Institute of Physics, Inc., New York, USA, 1986
3. Morse, P., Ingard, K.: “Theoretical Acoustics”, Princeton, New Jersey, USA, Princeton University Press, 1986
4. Vanderkooy, J.: "A Simple Theory of Cabinet Edge Diffraction", JAES, Vol. 39, No. 12, Dec. 1991

9. Addendum

```
|AkAbak Script - Dodecahedron model

Def_Const {                        |Dodecahedron geometric calculations
 a=0.11;                           |in meters, length of an edge of a pentagonal face
 p=5;  q=3;                        |Schlafli symbols {p,q} for regular polyhedra
 gr=2*arcsin((cos(pi/q)/sin(pi/p))); |dihedral angle after Coxeter
 grc=pi/2 - gr/2;                  |dihedral center angle
 r=(a/2)*(1/tan(pi/5));            |radius of an inscribed circle in one face
 doR1=r; doR2=doR1;                |distance to edge for diffraction
 b=r*tan(gr/2);                    |length of a vector from the geo- to a face center
 zed=b*cos(2*grc);                 |displacement of center points
 yed=b*sin(2*grc);                 |projection on the y-coordinate
 Vb=9.5e-3;                        |in m³, eff. inner volume of body
 Len=b;                            |length of Duct elements forming the enclosure
 Q_fo=0.5;                         |quality factor of enclosure

 |Mounting positions:
 x0=0;                  y0=0;                  z0=b;
 x1=yed*sin(rad(0));    y1=-yed*cos(rad(0));    z1=zed;
 x2=yed*sin(rad(72));   y2=-yed*cos(rad(72));   z2=zed;
 x3=yed*sin(rad(144));  y3=-yed*cos(rad(144));  z3=zed;
 x4=yed*sin(rad(216));  y4=-yed*cos(rad(216));  z4=zed;
 x5=yed*sin(rad(288));  y5=-yed*cos(rad(288));  z5=zed;
 x6=yed*sin(rad(-36));  y6=-yed*cos(rad(-36));  z6=-zed;
 x7=yed*sin(rad(36));   y7=-yed*cos(rad(36));   z7=-zed;
 x8=yed*sin(rad(108));  y8=-yed*cos(rad(108));  z8=-zed;
 x9=yed*sin(rad(180));  y9=-yed*cos(rad(180));  z9=-zed;
 x10=yed*sin(rad(252)); y10=-yed*cos(rad(252)); z10=-zed;
 x11=0;                 y11=0;                  z11=-b;

 |Mounting angles:
 VA0=0;  HA0=0;
 VA1=deg(arctan(y1/sqrt(sqr(x1) + sqr(z1))));
 HA1=deg(arctan(x1/z1));
 VA2=deg(arctan(y2/sqrt(sqr(x2) + sqr(z2))));
 HA2=deg(arctan(x2/z2));
 VA3=deg(arctan(y3/sqrt(sqr(x3) + sqr(z3))));
 HA3=deg(arctan(x3/z3));
 VA4=deg(arctan(y4/sqrt(sqr(x4) + sqr(z4))));
 HA4=deg(arctan(x4/z4));
 VA5=deg(arctan(y5/sqrt(sqr(x5) + sqr(z5))));
 HA5=deg(arctan(x5/z5));
 VA6=deg(arctan(y6/sqrt(sqr(x6) + sqr(z6))));
 HA6=-(180-deg(abs(arctan(x6/z6))));
 VA7=deg(arctan(y7/sqrt(sqr(x7) + sqr(z7))));
 HA7=180-deg(abs(arctan(x7/z7)));
 VA8=deg(arctan(y8/sqrt(sqr(x8) + sqr(z8))));
 HA8=180-deg(abs(arctan(x8/z8)));
 VA9=deg(arctan(y9/sqrt(sqr(x9) + sqr(z9))));
 HA9=180-deg(abs(arctan(x9/z9)));
 VA10=deg(arctan(y10/sqrt(sqr(x10) + sqr(z10))));
 HA10=-(180-deg(abs(arctan(x10/z10))));
 VA11=0;  HA11=180;
}
```

```
|Drive unit, type: Bose B901
Def_Driver  'Drv1'
  dD=9.35cm  dD1=30mm  tD1=11mm fp=4.5kHz
  Mms=4.95g  Cms=0.6e-3m/N  Rms=1Ns/m  Bl=2.1Tm
  Re=0.93ohm  Le=120uH  ExpoLe=0.618

System 'dodec'
  | Forward radiating loudspeakers
  Driver 'D1' Def='Drv1'  Node=10=11=100=31
  Radiator 'R1' Def='Drv1'  Node=100
    x={X0} y={Y0} z={Z0} HAngle={HA0} VAngle={VA0}  WEdge={doR1} HEdge={doR2}
  Driver 'D2' Def='Drv1' Node=11=12=101=32
  Radiator 'R2' Def='Drv1'  Node=101
    x={X1} y={Y1} z={Z1} HAngle={HA1} VAngle={VA1}  WEdge={doR1} HEdge={doR2}
  Driver 'D3' Def='Drv1' Node=12=13=102=33
  Radiator 'R3' Def='Drv1'  Node=102
    x={X2} y={Y2} z={Z2} HAngle={HA2} VAngle={VA2}  WEdge={doR1} HEdge={doR2}
  Driver 'D4' Def='Drv1'  Node=13=14=103=34
  Radiator 'R4' Def='Drv1' Node=103
    x={X3} y={Y3} z={Z3} HAngle={HA3} VAngle={VA3}  WEdge={doR1} HEdge={doR2}
  Driver 'D5' Def='Drv1'  node=14=15=104=35
  Radiator 'R5' Def='Drv1'  node=104
    x={X4} y={Y4} z={Z4} HAngle={HA4} VAngle={VA4}  WEdge={doR1} HEdge={doR2}
  Driver 'D6'  Def='Drv1'  node=15=0=105=36
  Radiator 'R6' Def='Drv1'  node=105
    x={X5} y={Y5} z={Z5} HAngle={HA5} VAngle={VA5}  WEdge={doR1} HEdge={doR2}
  | Rearward radiating loudspeakers
  Driver 'D7' Def='Drv1' node=10=21=106=37
  Radiator 'R7' Def='Drv1'  node=106
    x={X6} y={Y6} z={Z6} HAngle={HA6} VAngle={VA6}  WEdge={doR1} HEdge={doR2}
  Driver 'D8' Def='Drv1'   node=21=22=107=38
  Radiator 'R8' Def='Drv1'  node=107
    x={X7} y={Y7} z={Z7} HAngle={HA7} VAngle={VA7}  WEdge={doR1} HEdge={doR2}
  Driver 'D9' Def='Drv1' node=22=23=108=39
  Radiator 'R9' Def='Drv1'  node=108
    x={X8} y={Y8} z={Z8} HAngle={HA8} VAngle={VA8}  WEdge={doR1} HEdge={doR2}
  Driver 'D10' Def='Drv1'  node=23=24=109=40
  Radiator 'R10' Def='Drv1'  node=109
    x={X9} y={Y9} z={Z9} HAngle={HA9} VAngle={VA9}  WEdge={doR1} HEdge={doR2}
  Driver 'D11' Def='Drv1'  node=24=25=110=41
  Radiator 'R11' Def='Drv1'  node=110
    x={X10} y={Y10} z={Z10} HAngle={HA10} VAngle={VA10}  WEdge={doR1} HEdge={doR2}
  Driver 'D12' Def='Drv1'  node=25=0=111=42
  Radiator 'R12' Def='Drv1'  node=111
    x={X11} y={Y11} z={Z11} HAngle={HA11} VAngle={VA11}  WEdge={doR1} HEdge={doR2}

  |Enclosure build up by Duct elements
  Duct 'Du1'  node=30=31  SD={Vb/(Len*13)}  QD/fo={Q_fo}  Len={Len}
  Duct 'Du2'  node=30=32  SD={Vb/(Len*13)}  QD/fo={Q_fo}  Len={Len}
  Duct 'Du3'  node=30=33  SD={Vb/(Len*13)}  QD/fo={Q_fo}  Len={Len}
  Duct 'Du4'  node=30=34  SD={Vb/(Len*13)}  QD/fo={Q_fo}  Len={Len}
  Duct 'Du5'  node=30=35  SD={Vb/(Len*13)}  QD/fo={Q_fo}  Len={Len}
  Duct 'Du6'  node=30=36  SD={Vb/(Len*13)}  QD/fo={Q_fo}  Len={Len}
  Duct 'Du7'  node=30=37  SD={Vb/(Len*13)}  QD/fo={Q_fo}  Len={Len}
  Duct 'Du8'  node=30=38  SD={Vb/(Len*13)}  QD/fo={Q_fo}  Len={Len}
  Duct 'Du9'  node=30=39  SD={Vb/(Len*13)}  QD/fo={Q_fo}  Len={Len}
  Duct 'Du10' node=30=40  SD={Vb/(Len*13)}  QD/fo={Q_fo}  Len={Len}
  Duct 'Du11' node=30=41  SD={Vb/(Len*13)}  QD/fo={Q_fo}  Len={Len}
  Duct 'Du12' node=30=42  SD={Vb/(Len*13)}  QD/fo={Q_fo}  Len={Len}
  Enclosure  'E1'  Node=30  Vb={Vb/13}  Qb/fo={Q_fo}  Lb={Len}
    Len=1mm  SD=5cm2  QD/fo=0.007  WEdge={doR1} HEdge={doR2}
```

Fig. 1 Photo of dodecahedron

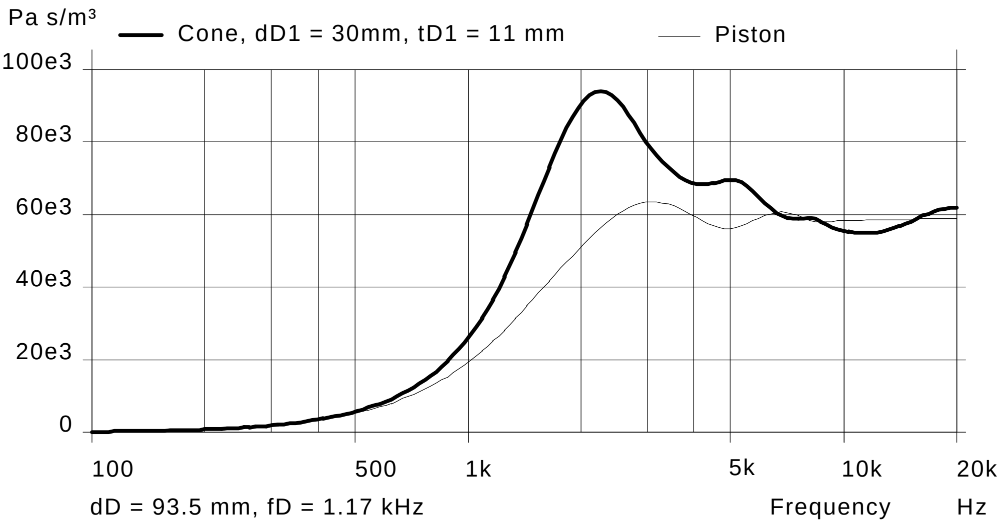

Fig. 2 Radiation impedance of piston and cone diaphragm

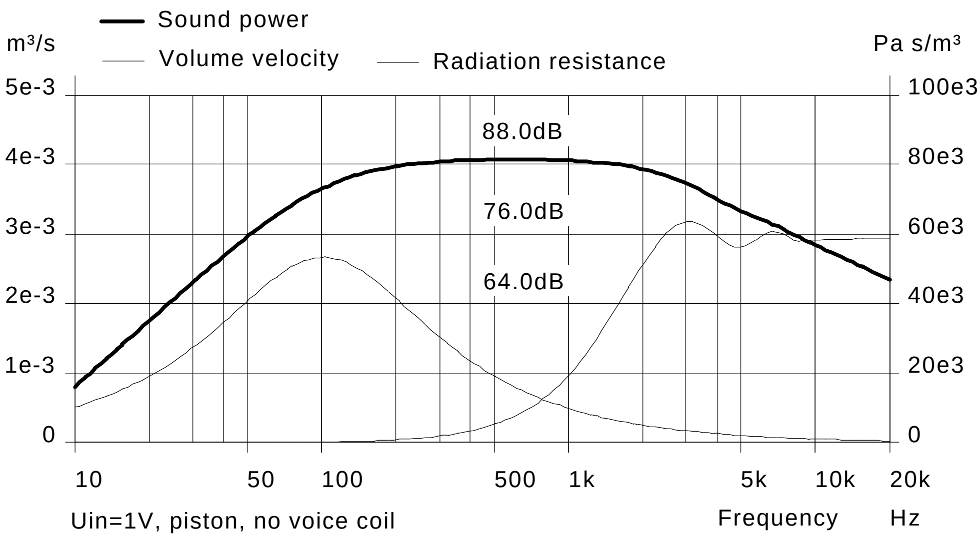

Fig. 3 Velocity, radiation resistance and sound power level of piston diaphragm

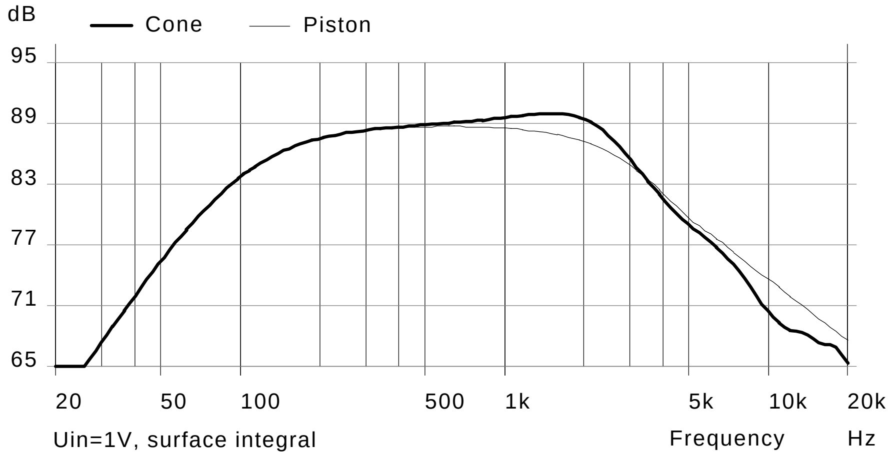

Fig. 4 Sound power level of piston and cone diaphragm

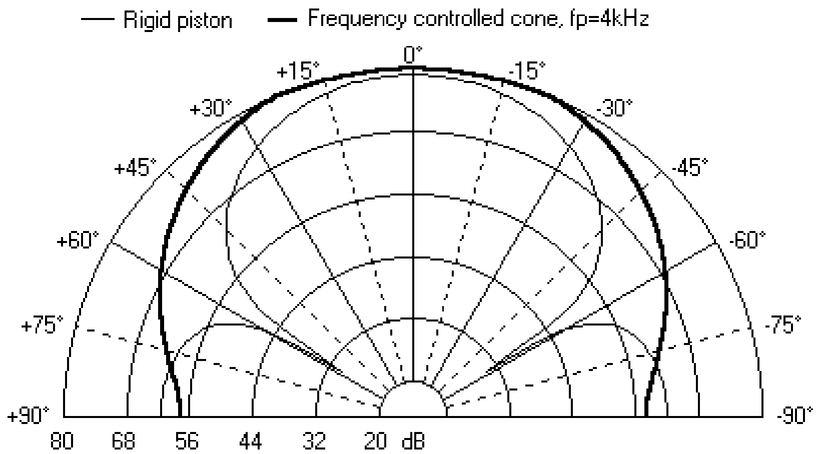

Fig. 5 Directivity pattern. Rigid cone and frequency controlled cone

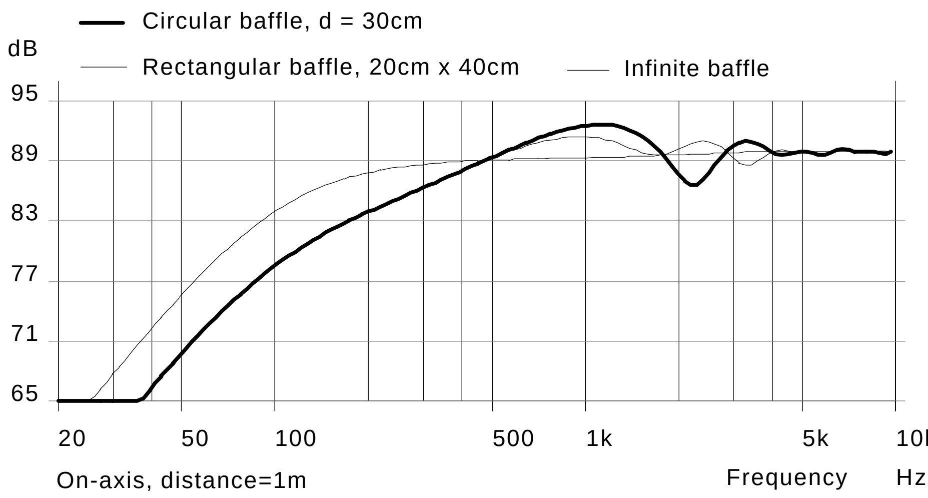

Fig. 6 SPL. Single driver mounted in the center of
a circular and a rectangular baffle (1:2).
(piston and voice coil reactance switched off to demonstrate the effect)

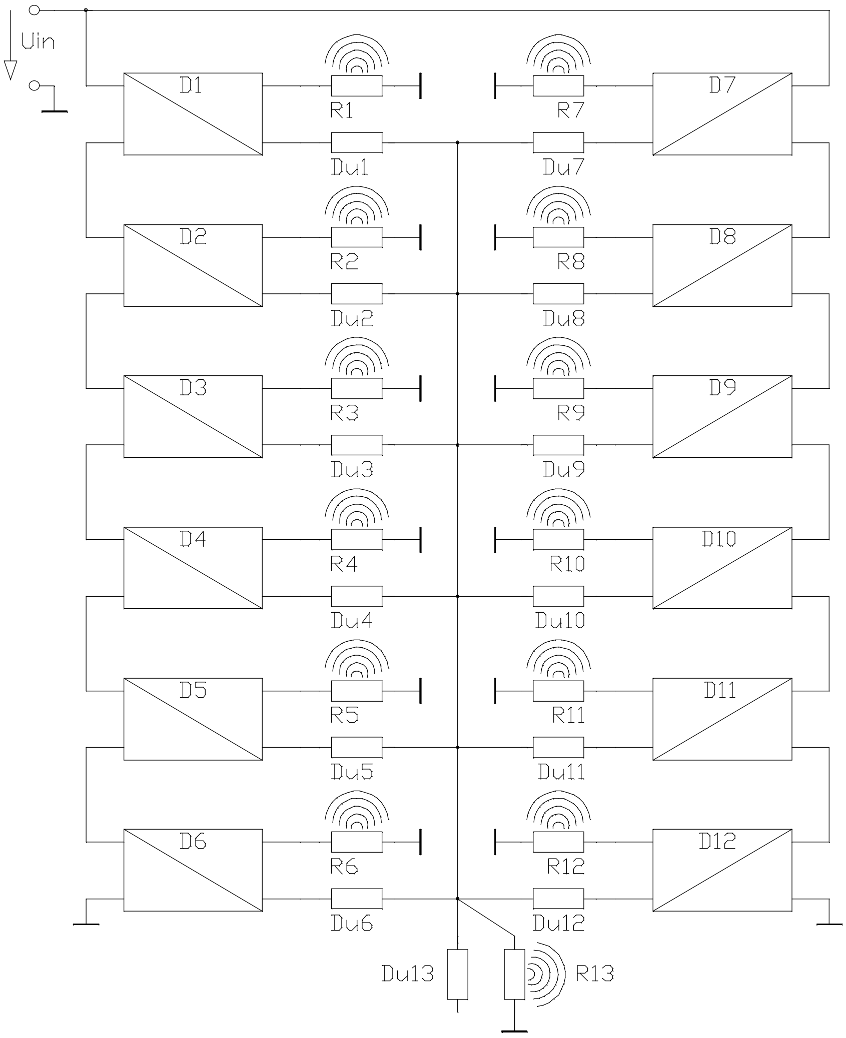

Fig. 7 Equivalent circuit.
Drivers: D1...D12. Ducts: Du1...Du13.
Radiation impedance and radiation: R1...R13

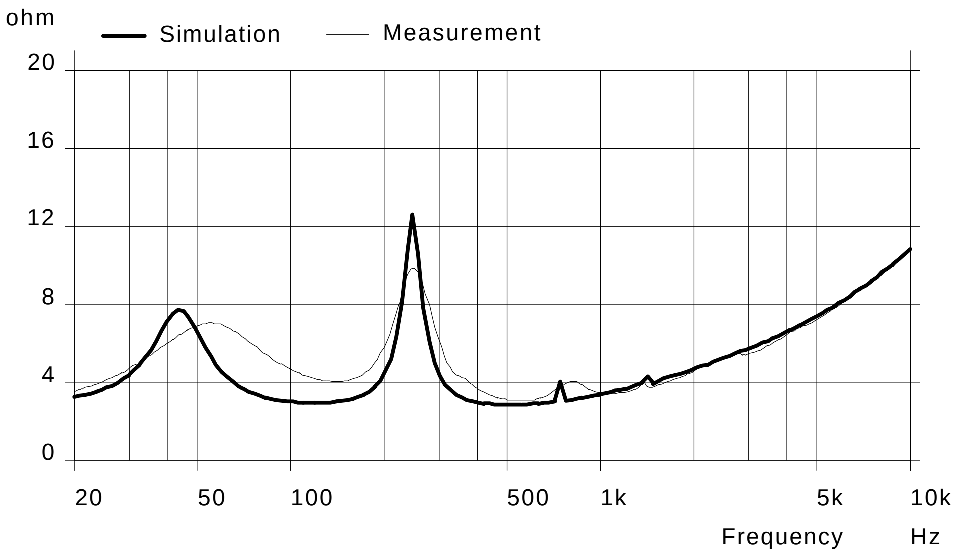

Fig. 8 Electrical input impedance
measurement and simulation

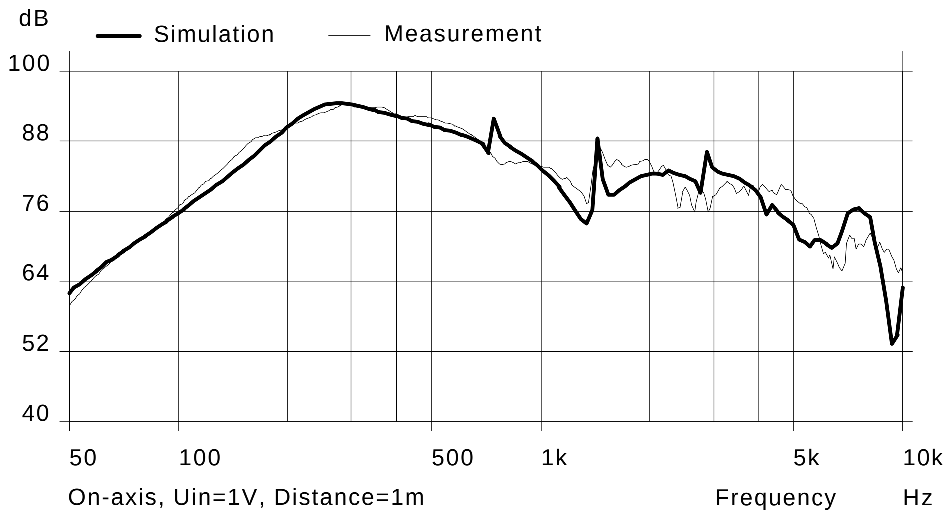

Fig. 9 On-axis SPL of dodecahedron loudspeaker,
simulation and measurement

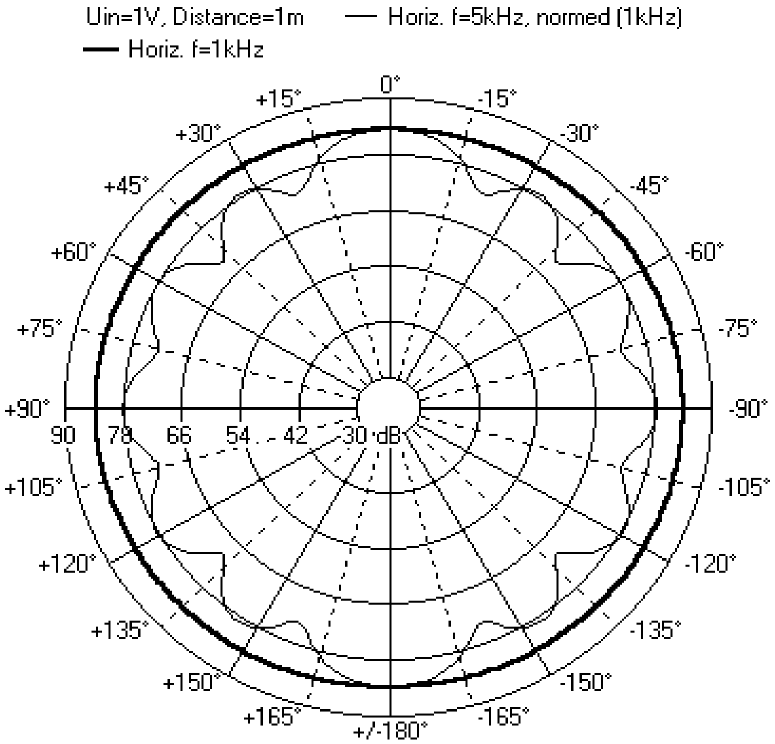

Fig. 10 Directivity of dodecahedron loudspeaker

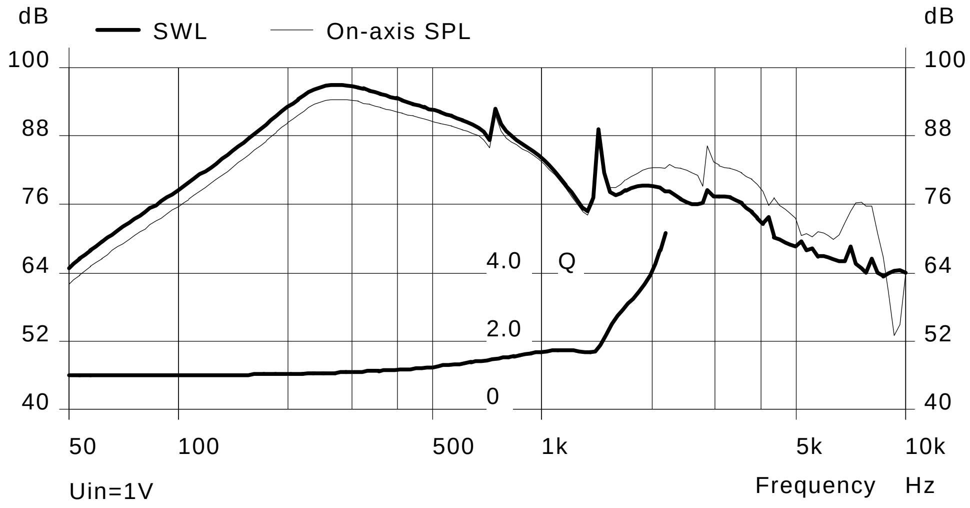

Fig. 11 Sound power level (SWL), Sound pressure level (SPL) and directivity factor (Q) of dodecahedron loudspeaker

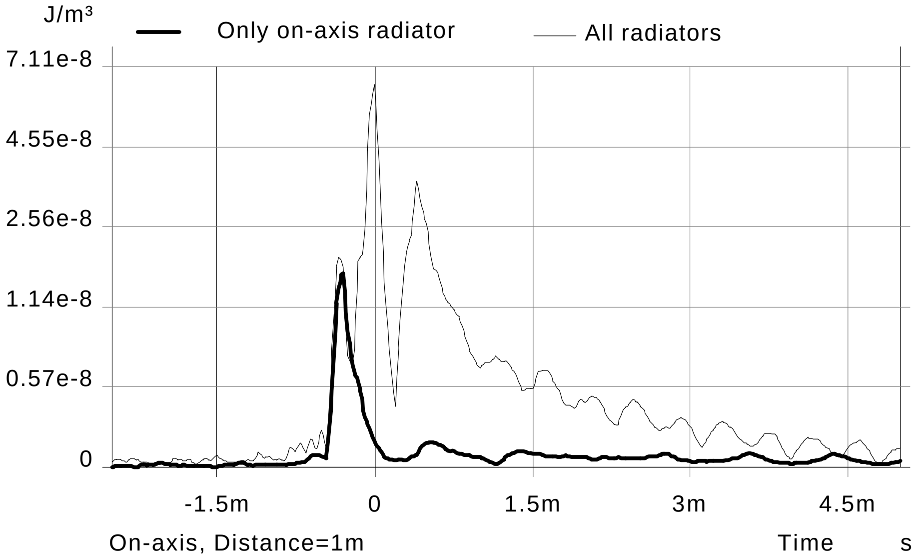

Fig. 12 ETC of SPL
Radiation of a single driver and of multiple drivers